In: Advances in Chemistry Research. Volume 10 ISBN 978-1-61324-018-2
Editor: James C. Taylor, pp. 341-359

Chapter 11

COMPARISON BETWEEN ZIRCONIA AND ALUMINA SUPPORTS FOR NICKEL-BASED CATALYSTS FOR HYDROGEN PRODUCTION

Maria do Carmo Rangel[1]*, Guillermo Paternina Berrocal[1], Cristhiane G. Maciel[2] and José Mansur Assaf[2]

[1]GECCAT, Instituto de Química, Universidade Federal da Bahia. Campus Universitário de Ondina. 40155-290, Salvador, Bahia, Brazil

[2]Laboratório de Catalise, Departamento de Engenharia Química, Universidade Federal de São Carlos, São Paulo, Brazil

ABSTRACT

Alumina and zirconia, as well as a zirconium and aluminum-containing solid, were compared as supports for nickel-based catalysts to produce hydrogen by steam reforming and autothermal reforming of methane. Samples were prepared by precipitating aluminum and zirconium compounds, followed by the impregnation of the supports with nickel nitrate (15 %) and characterized by FTIR, TG and DTA, XRD, TPR and specific surface area and porosity measurements. The catalysts were evaluated in steam reforming and autothermal reforming of methane in the range of 450-750°C. Zirconia-supported nickel showed the monoclinic and tetragonal phases while alumina-supported nickel showed the gamma phase; the aluminum and zirconium-containing solid showed the tetragonal phase and gamma-alumina, indicating that alumina stabilized tetragonal zirconia. Nickel oxide (NiO) was found in all solids. All catalysts were active in both steam reforming and authothermal reforming and the conversion increased with temperature. For both reactions, alumina and zirconia produced catalysts with similar activities and selectivities to hydrogen, the mixed catalyst showed the lowest values. These findings were related to the ability of zirconia of favoring the reduction of nickel particles while alumina is responsible for the high specific surface area, both related to the increase of nickel active sites. Also, zirconia led to catalysts more active to water gas

* Corresponding author: mcarmov@ufba.br.

shift reaction than alumina. The H_2/CO ratio can be adjusted by the kind of the support and the reaction temperature.

INTRODUCTION

Hydrogen is expected to become an important source of energy in the future, mainly due to its potential use in fuel cells [1, 2], besides the possibility of being burned directly in an internal combustion engine [3]. In addition, it is largely used in chemical, petrochemical and food industries, as well as in electronics and in oil refining, among other applications. In chemical and petrochemical industries, it is widely used for the production of ammonia, hydrogen peroxide, alcohols and others [4]. In refineries, the most application is concerning to hydrodesulphurization [5], while in food industry it is especially used in hydrogenation of fats and oils [6]. Also, in steel and electronics industries it is used in the manufacture of electronic devices [7].

Currently, steam reforming of natural gas is by far the most important route for producing hydrogen worldwide, while partial oxidation, autothermal reforming and dry reforming have also been considered [8-13]. All these processes are also attractive for the generation of synthesis gas (syngas) with different carbon monoxide to hydrogen ratios, used for different purposes [8]. The reforming with carbon dioxide also called dry reforming, for instance, produces syngas with a ratio H_2/CO of one, which is particularly suitable for Fisher-Tropsch reaction [14]. This process has attracted an increasing interest in last years because it consumes carbon dioxide and methane, two greenhouse gases. On the other hand, partial oxidation is an exothermic process in which hydrocarbons are converted to synthesis gas with H_2/CO ratio of two, through the incomplete combustion by oxygen [15]. It has the disadvantage of requiring an external source of oxygen. Steam reforming, in turn, is adequate to produce a H_2/CO ratio of three, while the ratio can be adjusted by changing the process condition for autothermal reforming [16]. This process combines partial oxidation with steam reforming and thus decreases the energy expenditure, since the heat required for the second reaction is provided by the first one. This process, as the partial oxidation, has the disadvantage of requiring a source of oxygen, which increases the operational costs [9]. As a whole, the most widely used catalysts for all reforming processes are based on nickel, which have low cost and are sufficiently active, as compared to noble metals, although they show the disadvantage of coke formation [10, 17-20].

Other processes for hydrogen production include pyrolysis and plasma reforming of hydrocarbons as well as ammonia reforming. The pyrolysis of organic materials can be performed in the absence of water or oxygen, which prevents the formation of carbon monoxide and dioxide, avoiding subsequent steps such as the water gas shift reaction; in addition, the process produces valuable clean carbon [21]. In plasma reforming, the reactions involved are the same as those of conventional reforming, being the energy provided artificially by a plasma [22]. The ammonia reforming was originally proposed for fuel cell applications [23]. Several catalysts have been used in this process like iron oxide, molybdenum, ruthenium and nickel [9, 23]. Other routes for producing hydrogen are derived from different treatments of biomass, such as gasification, conversion to liquid fuels by supercritical fluid extraction, liquefaction, hydrolysis and others. Hydrogen can also be produced by electrolysis of water [9].

Among these processes, the steam reforming of methane is the most economical and used route to produce hydrogen, this process has been optimized for several decades [17, 24, 25]. The main reactions are the conversion of methane into carbon monoxide and hydrogen (Eq. 1) and the water gas shift reaction, WGSR (Eq.2) [10, 11, 19, 20, 26].

$$CH_4 + H_2O \rightleftharpoons CO + 3H_2 \qquad \Delta H^\circ_{298} = 206\ kJ.mol^{-1} \qquad (1)$$

$$CO + H_2O \rightleftharpoons CO_2 + H_2 \qquad \Delta H^\circ_{298} = -41\ kJ.mol^{-1} \qquad (2)$$

The steam reforming reaction (Eq. 1) is highly endothermic, being favored by low pressures and high temperatures. However, the industrial process is operated at high pressures and temperatures (800 °C and 30 bar), in order to achieve rates for economical purposes. From the stoichiometry, one water molecule is consumed per carbon atom but, in commercial operations, the catalysts tend to favor reactions that produce coke and then H_2O/CH_4 molar ratios in the range of 2.5 to 3.0 are often used [17]. For modern plants operating at high temperatures and low steam/gas ratios, efficiencies around of 94 % of the calculated value are achieved, indicating that the existing technology for producing hydrogen by steam reforming of methane has evolved significantly, resulting in a more efficient process with reduced operating costs [24].

The commercial catalyst, traditionally used in steam reforming of natural gas, is based on nickel (12 to 20 %) supported on a refractory material such as alpha alumina containing alkaline promoters, like potassium or calcium, which decrease coke deposition and improve the stability of the catalyst [9, 17, 19, 20]. Noble metals such as iridium, platinum, palladium, rhodium and ruthenium, which are less affected by coke deposition, have also been used [10, 25, 26]. Because of the severity of the process, the support should be mechanically and thermally resistant, with specific surface area high enough to promote a high metal dispersion; also, it should not be able to catalyze secondary reactions, especially those forming coke [25]. Several supports used in steam reforming of methane have been proposed such as alumina, silica, magnesia, zirconia, titania, ceria, hafnia, thoria, lanthana and tantalum oxide, as well as strontium, barium and calcium oxide, silicon carbide, barium phosphate and calcium aluminate [10, 11, 20, 25].

In recent years, there has been a growing interest for partial oxidation of methane (Eq. 3), which is moderately exothermic [15, 18, 27, 28]. The reaction is often described by two mechanisms, direct and indirect. The first case involves the initial formation of carbon monoxide and hydrogen which desorb from the catalyst, before being converted to total oxidation products (carbon dioxide and water). In the indirect synthesis, methane is completely oxidized into carbon dioxide and water, which are then reformed to produce syngas [29].

$$CH_4 + 1/2O_2 \rightleftharpoons CO + 2H_2 \qquad \Delta H^\circ_{298} = -36\ kJ/mol \qquad (3)$$

The partial oxidation of methane has some advantages compared to steam reforming, such as the lower energy consumption due to exothermic reaction, allowing the use of the heat generated in the process. Also, reactors with lower volume and weight can be used by

providing flexibility regarding production scale, as well as a more rapid response to variations of operating conditions [17, 29, 30]. A disadvantage of this process is the need for large amounts of oxygen continuously, which requires investment in building a plant for the generation of this product [17].

Several catalysts were evaluated in this reaction including the nickel-based ones, which showed a strong tendency to sintering and carbon formation, thus requiring stabilization by small amounts of calcium oxide, potassium or sodium bicarbonate. The catalysts based on noble metals have also been investigated, showing higher activities than the nickel catalysts. Among them, iridium, platinum, palladium, rhodium and ruthenium have showed the best performances but show the disadvantage of high cost [28, 31].

In recent years, the combination of steam reforming and partial oxidation of hydrocarbons has been proposed as an alternative route for hydrogen production, taking the advantages of these two processes. This results in the autothermal reforming (Eq. 4), whose main advantage is the exothermic and endothermic reactions that occur simultaneously, minimizing the energy cost of the plant, without requiring an external source of heat for the reactor [17, 31]. In this case, there is a thermal zone in which the heat generated in the exothermic reaction of partial oxidation is used in steam reforming. The temperature profile in the reactor is characterized by a marked increase in the thermal zone and then progressively decreases the temperature in the area due to the endothermic reactions. To properly operate the autothermal reforming process, there is a need to control the amount of oxygen, methane and steam, with the aim of controlling the reaction temperature and the kind of products obtained, as well as to prevent coke formation [9]. During operation, temperatures can reach values as high as 2000 to 2200 ^{o}C, in the combustion zone and 1000 to 1200 ^{o}C, in the catalytic zone. For fuel cell applications, a compact arrange has been proposed, in which both the partial oxidation and the steam reforming occur simultaneously on the catalyst bed. In other arrange, there are separate sections, in the first (combustion chamber) the non-catalytic partial oxidation occurs while in the second section the steam reforming occurs on a catalytic bed [32].

$$2\,CH_4 + H_2O + \tfrac{1}{2}\,O_2 \rightleftharpoons 2\,CO + 5\,H_2 \qquad (4)$$

Despite the autothermal reforming has been originally used to maximize the amount of hydrogen in ammonia plants, it can be conveniently used for the production of synthesis gas with high or low content of carbon monoxide [31]. It has been demonstrated [16], for instance, that increasing the H_2O/CH_4 molar ratio the hydrogen production is increased, since steam reforming reaction is favored while the increasing O_2/CH_4 molar ratio favors the carbon monoxide formation, because the reaction oxidation is favored.

The catalysts used in autothermal reforming of methane are the same used in steam reforming and partial oxidation of methane. Thus, catalysts based on nickel or cobalt, supported on a refractory material such as alumina or magnesium aluminate promoted with alkali or alkaline earth, are often used. Also, noble metals such as rhodium, ruthenium, palladium, platinum and rhenium supported on alumina or on rare earth oxides, especially cerium oxide, have been show good performances [12].

In a previous work [11], we have found that the addition of aluminum to zirconia-supported nickel is beneficial to the catalyst, increasing the activity in the partial oxidation of

methane. In the present work, zirconia and alumina-based supports for nickel catalysts were compared in the hydrogen production through steam reforming and autothermal reforming of methane. The study aims to develop efficient catalysts to produce high pure hydrogen.

EXPERIMENTAL

Alumina, zirconia and aluminum and zirconium-containing solid (Al/Zr (molar)= 1) were used as catalytic supports. For alumina preparation (Al sample), an aqueous solution of aluminum nitrate (1 M, 250 mL) was added simultaneously with an aqueous solution of ammonium hydroxide (8.2% v/v) to water, at room temperature. During reaction, the system was kept under stirring and the final pH was 9. The sol was matured for 24 h and then centrifuged at 2800 rpm, for 5 min. The gel obtained was washed with an aqueous solution 1 % v/v of ammonium hydroxide to remove nitrate ions and centrifuged again. The sample was dried at 120 ^{o}C, for 24 h and calcined (10 °C.min^{-1}) at 750 °C, for 2 h, under air flow (100 mL.min^{-1}). In the preparation of zirconium oxide (Zr sample), an aqueous solution of zirconium oxychloride (1 M, 250 mL) was added simultaneously with an aqueous solution of ammonium hydroxide (8.2% v/v) to water. Then, the procedure followed the same steps described for alumina preparation. The aluminum and zirconium-containing solid (AZ sample) was prepared by the same method, by adding simultaneously aqueous solutions of aluminum nitrate (1 M), zirconium oxychloride (1 M) and ammonium hydroxide (8.2% v/v) to water.

The catalysts were prepared by impregnating the supports with nickel nitrate solutions in order to obtain 15 % of the metal. The support was dispersed in a nickel nitrate solution (1.4 mL of water/g of support) and stirred at 80 ^{o}C, for 2 h. The solid was then dried at 120 ºC, for 24 h and calcined (10 ^{o}C.min^{-1}) at 750 ºC, for 2 h, under a flow of 100 mL. min^{-1}.

The precursors of the supports were characterized by thermogravimetry, differential thermal analysis and Fourier transform infrared spectroscopy. The supports and catalysts were characterized by X-ray diffraction, specific surface area and porosity measurements, Fourier transform infrared spectroscopy and temperature programmed reduction.

The experiments of thermogravimetry (TG) and differential thermal analysis (DTA) were performed on the support precursors, in order to follow the metallic oxide production and its stability. The sample (0.005 g) was heated (10 ^{o}C.min^{-1}) in a TGA/SDTA 851 Mettler Toledo equipment, under flowing air (50 mL.min^{-1}) in the range of 25 to 1000 °C. The presence of nitrate species in solids was followed by Fourier transform infrared spectroscopy (FTIR), which was carried out in a Perkin Elmer spectrometer model Spectrum One, in the range of 500-4000 cm^{-1}, using discs of the samples dispersed in potassium bromide.

The X-ray diffractograms were obtained in a Shimadzu model XRD-6000 equipment, operating with a CuKα (λ= 1.5420 Å) radiation in the 2θ range between 10 and 80 degrees, with a scan rate of 2^{o}. min^{-1}. The specific surface area measurements were performed in an ASAP 2020 Micromeritics apparatus. Before analysis, the sample (approximately 0.3 g) was evacuated (10 μmHg), for 30 min and heated at 200 ^{o}C, for 60 min, under nitrogen flow. To calculate the specific surface area and porosity, the methods of Brunauer-Emmett-Teller (BET) and of Barrett-Joyner-Halenda (BJH) were used, respectively.

The experiments of temperature programmed reduction were performed in a Micromeritics apparatus model TPD/TPR 2900. The sample (0.3 g) was previously heated (10 ^{o}C.min^{-1}) up to 160 °C, under nitrogen flow, for 30 min. The sample was cooled to room temperature and analyzed using a mixture of 5 % H_2/N_2, by heating the reactor up to 1000 °C at a rate of 10 ^{o}C.min^{-1}.

The catalysts were evaluated in steam reforming and in autothermal reforming of methane. The steam reforming was performed in a fixed bed reactor, using 0.1 g of sample, at 1 atm and temperatures ranging from 450 to 750 ^{o}C, under a flow of methane (20 mL.min^{-1}) and steam (7.1 g.h^{-1}). Before reaction, the solids were reduced *in situ* at 700 °C, under hydrogen flow (30 mL.min^{-1}), for 2 h. The reaction products were analyzed online in a Varian model GC-3800 gas chromatograph equipped with two thermal conductivity detectors and Porapaq Q and molecular sieve 13X separation packed columns.

The same experimental set was used for evaluating the catalysts in autothermal reforming, at different temperatures ranging from 450 to 750 ^{o}C and 1 atm, under methane (20 mL.min^{-1}), air (47 mL.min^{-1}) and steam (3.9 g.h^{-1}) flow. Before reaction, the samples were reduced *in situ* at 700 °C, under hydrogen flow (30 mL.min^{-1}), for 90 min. The reaction products were analyzed online as above described.

RESULTS AND DISCUSSION

Figure 1 shows the thermogravimetry (TG) and derivative thermogravimetry (DTG) curves for the support precursors. For aluminum-containing solids (Al and AZ samples), three stages of weight loss were noted while zirconium-based solid (Zr sample) showed two steps. For all cases the first weight loss, in the range of 25 to 120 °C (centered at around 95 °C), is associated with the removal of water and volatiles adsorbed on the solid [10, 33]. This process is endothermic, as shown by the DTA curves, displayed in Figure 2.

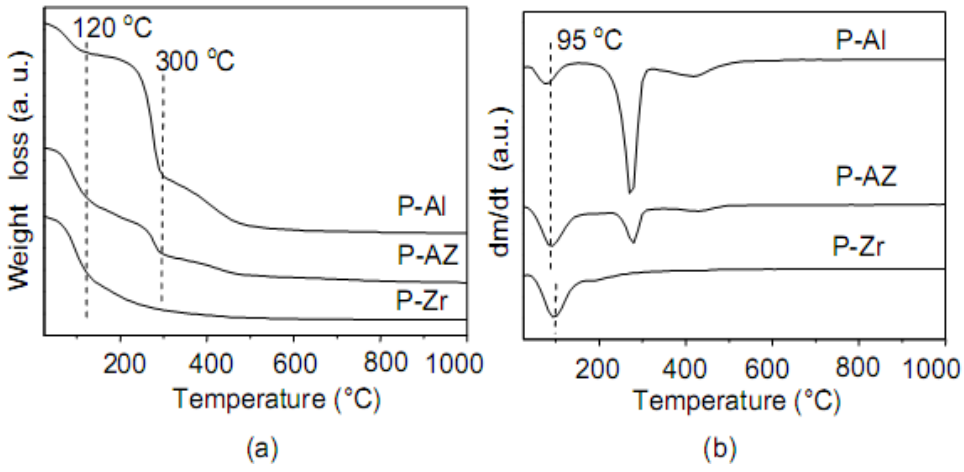

Figure 1. Curves of (a) thermogravimetry and (b) derivative thermogravimetry of support precursors (P). Al sample: aluminum oxide. Zr sample: zirconium oxide. AZ sample: aluminum and zirconium-based solid (Al/Zr (molar) = 1).

For aluminum-based solids (Al and AZ samples), the second weight loss from 120 to 300 °C, associated with an endothermic peak in DTA curve, is related to dehydroxylation of aluminum hydroxide, producing boehmite and bayerite, which is followed by loss of water and of residual nitrate species from the precursor salt [10, 33]. The third weight loss above 300 °C, related to a broad exothermic peak in DTA curve, can be attributed to the formation of different types of transition alumina such as γ-alumina, which is formed at 450 ^{o}C and δ-alumina, produced at around 900 °C [10, 34].

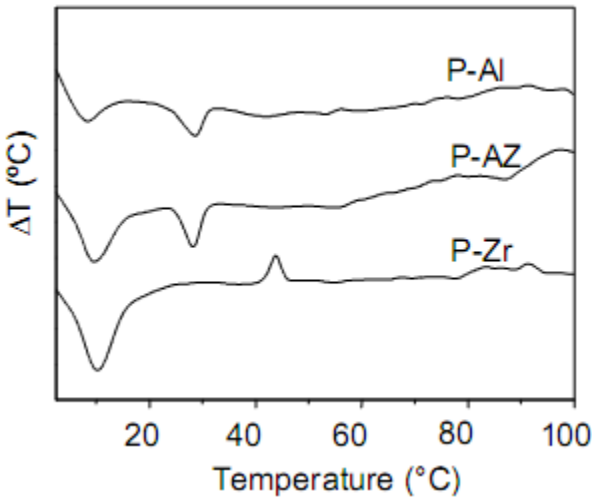

Figure 2. DTA curves of the support precursors (P). Al sample: aluminum oxide. Zr sample: zirconium oxide. AZ sample: aluminum and zirconium-based solid (Al/Zr (molar) = 1.

For zirconium-based sample (Zr), the second loss in the range of 120 to 475 °C is associated with formation of zirconium oxide [35]. In DTA curve, an exothermic peak centered at 440 ° C is related to the production of zirconium oxide, while the other peak at temperatures higher than 700 ^{o}C can be ascribed to the transition from monoclinic to tetragonal phase [36].

For all samples, a total weight loss of 23 to 48 % was noted, which decreased with increasing amount of zirconium, since that less water was lost. Thus, the solid containing only aluminum showed the largest weight loss (47.7 %) followed by aluminum and zirconium-based solid (30.7 %) and the sample containing only zirconium (23.5 %).

FTIR spectra of precursors and supports (not shown) displayed a broad band above 3000 cm^{-1}, related to vibrations of hydroxyl groups and a band at 1650 cm^{-1}, associated to the deformation vibration of water molecules adsorbed on the solids [37]. For the precursors, it can be noted a band in 1380 cm^{-1}, characteristic of nitrate and chloride species [37], indicating that the rinsing of gel, during sample preparation, was insufficient to remove these groups from the solids. For the spectra of the supports, these bands were not found for AZ sample, indicating these species were removed during calcination. For the other cases, this band was weaker, as compared to the precursors, indicating that these species were partially removed from the solid, during calcination. Moreover, the spectra of aluminum-based support precursors showed a band at 1050 cm^{-1} which can be attributed to deformation vibrations of hydroxyl groups, characteristic of boehmite and a band at about 740 cm^{-1}, typical of

stretching vibration of Al-O bond, which can be associated to oxygen atoms in octahedral coordination in boehmite [38].

Figure 3 shows the spectra for precursors and catalysts. Also, the absorptions at 1640 and above 3000 cm^{-1}, related to deformation and stretching vibrations of water molecules, respectively and a band at 1380 cm^{-1} characteristic of nitrate species [37], appear weaker for the catalysts, as compared to the precursors, indicating that a small amount of these species remains in the catalysts.

The X-ray diffraction of supports and catalysts are shown in Figure 4. Pure zirconia (Zr sample) shows a profile typical of monoclinic and tetragonal phases, in agreement with previous studies [11, 39]. On the other hand, the diffractogram of alumina (Al sample) showed peaks related to γ-alumina. It was found that aluminum stabilized the tetragonal phase of zirconia, since the AZ sample showed no peak related to monoclinic phase, in accordance with previous work [11]. Also, γ-alumina was found in this sample.

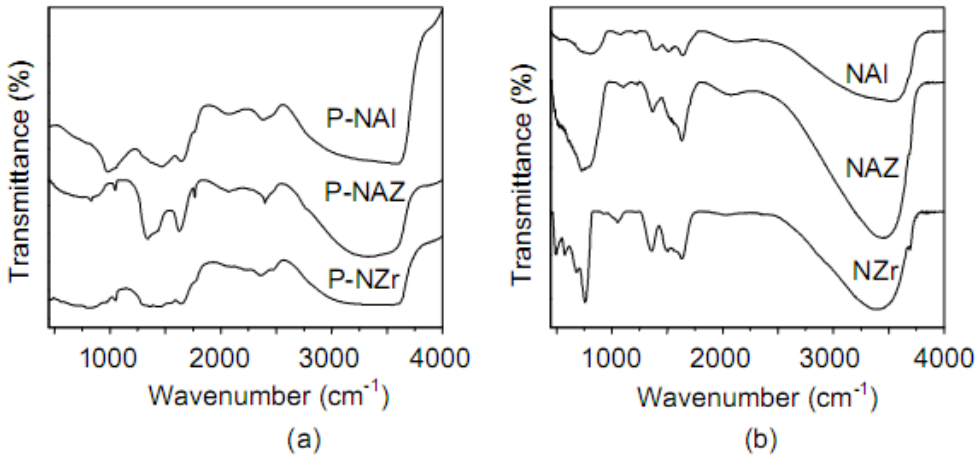

Figure 3. FTIR spectra of (a) precursors and of (b) catalysts. NAl and NZr samples: nickel on alumina and on zirconia, respectively. NAZ sample: nickel aluminum and zirconium sample (Al/Zr = 1).

For the zirconium-based catalyst (NZr sample), tetragonal and monoclinic phases were found, while for aluminum-based catalyst (NAl sample) γ-Al_2O_3 was detected. In the case of aluminum and zirconium sample (NAZ), tetragonal zirconia and γ-Al_2O_3 were found. For both cases, it was not possible to detect nickel aluminate because of the coincidence of the peaks of this phase with the peaks of γ-Al_2O_3. Nickel oxide (NiO) was found for all catalysts.

The values of specific surface areas of supports and catalysts are shown in Table 1. Alumina (Al sample) showed the highest value while zirconia showed the lowest one, the zirconium and aluminum-based solid showed a value close to zirconia. After nickel impregnation and calcination, the specific surface area decreased, possibly due to the blockage of pores by nickel compounds.

The nitrogen adsorption isotherms of the supports are shown in Figure 5. Aluminum-based samples (A and AZ1 samples) showed a Type II isotherm with a hysteresis loop, characteristic of macroporous materials with mesopores [40]. On the other hand, the curve of the sample of zirconia showed the profile of the Type III isotherm with a narrow hysteresis loop at high pressures, indicating the presence of some mesopores interparticles.

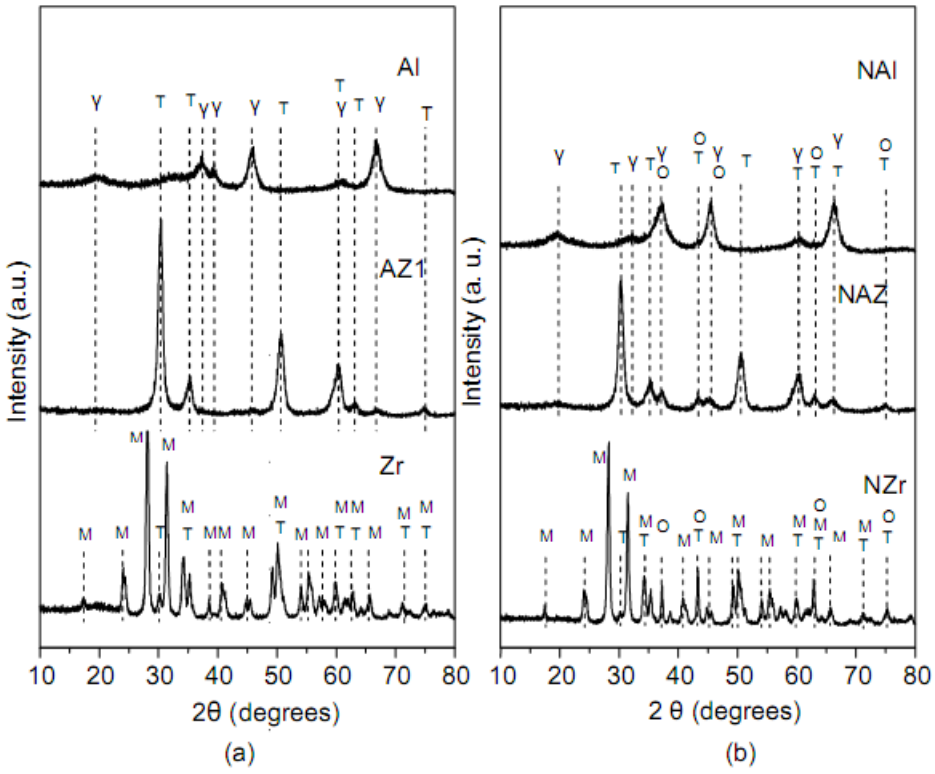

Figure 4. X-ray diffraction patterns of (a) supports and (b) catalysts. A sample: alumina. Z sample: zirconia. AZ sample: aluminum and zirconium-based solid (Al/Zr= 1). The letter N indicates the presence of nickel. O= nickel oxide; M= monoclinic phase; T= tetragonal phase; γ=gama-alumina.

Table 1. Specific surface areas of supports and catalysts. Zr sample: zirconia. Al sample: alumina. AZ sample: zirconium and aluminum-based solid (Al/Zr= 1). The letter N indicates the presence of nickel

Sample	Al	AZ	Zr	NAl	NAZ	NZr
Sg ($m^2.g^{-1}$)	178	99	91	129	59	24

Figure 6 shows the TPR curves of catalysts. For the alumina-based sample (NAl) two peaks were noted, a small one at 367 °C, related to reduction of nickel in weak interaction with the support [41] and a broad peak above 650 ºC, associated to reduction of nickel in strong interaction with the support, possibly as nickel aluminate, $NiAl_2O_4$, in accordance with other works [40-42]. For zirconia-based catalyst (NZr), a broad peak from 320 to 600 ^oC was detected, related to nickel reduction; it occurred at lower values, as compared to alumina-based sample, indicating that zirconium decreased the interaction of nickel with the support and then makes its reduction easier. The aluminum and zirconium-based catalyst (NAZ sample) showed a broad peak from 450 to 950 ^oC, related to nickel reduction, which occurred at intermediate temperatures, as compared to the other samples. It means that this solid is more reducible than alumina-supported nickel, probably due to a decrease of the production of nickel aluminate.

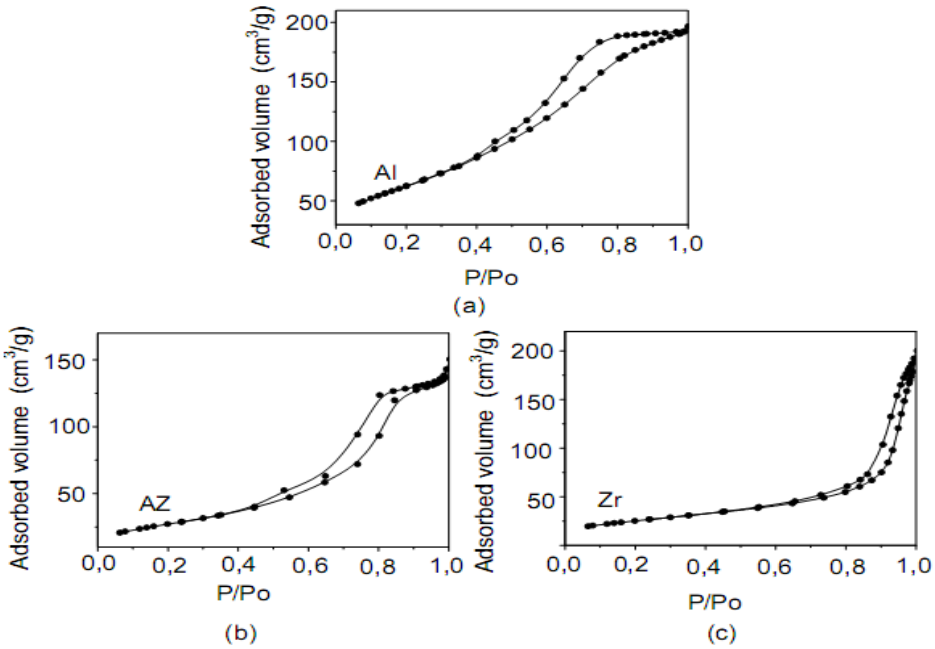

Figure 5. Nitrogen adsorption-desorption isotherms for (a) alumina (Al sample), (b) zirconia and aluminum-based solid (AZ sample) and (c) zirconia (Zr sample).

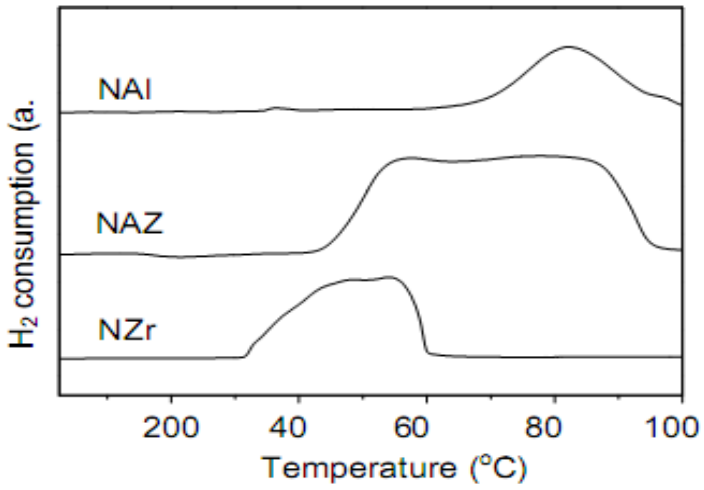

Figure 6. TPR profiles of the catalysts. NAl sample: nickel on alumina. NZr sample: nickel on zirconia. NAZ sample: nickel on aluminum and zirconium-based solid (Al/Zr (molar) = 1).

The methane conversion on the catalysts as a function of temperature, during steam reforming, is shown in Figure 7. It can be seen that the conversion increased with temperature for all catalysts. Zirconia-supported nickel and alumina-supported nickel showed similar activities, the first one leading to higher values at higher temperatures. Zirconia-supported nickel has the lowest specific surface area but is the most reducible sample; on the other hand, alumina-supported nickel has the highest specific area and is the least reducible. They showed similar conversions, suggesting that they produce a similar number of active sites, by

compensating the specific surface area and the ability to produce metallic nickel, which is supposed to be the active phase. On the other hand, the aluminum and zirconium-containing sample has an intermediate specific surface area and reducibility; in this case, it seems that the low specific surface area combined to low reducibility resulted in a decrease of active sites and thus in the activity.

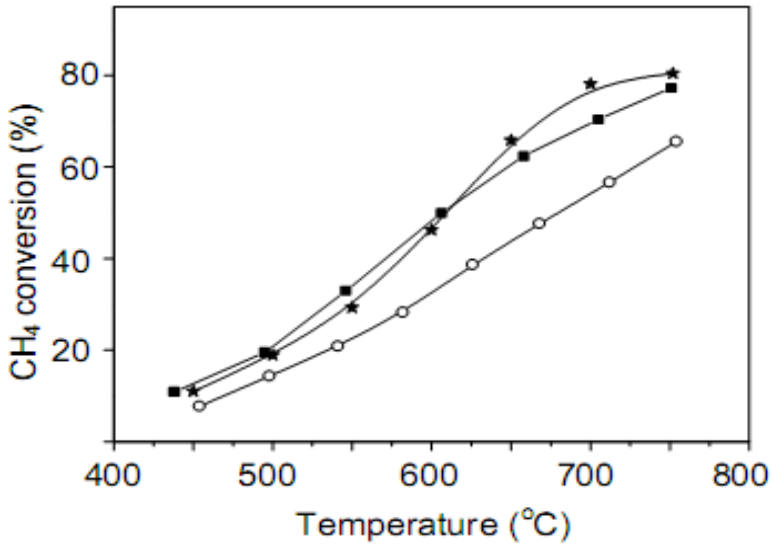

Figure 7. Methane conversion as a function of temperature in steam reforming over the catalysts. NAl sample (■): alumina-supported nickel. NZr sample (★): zirconia-supported nickel. NAZ sample (○): nickel supported on aluminum and zirconium solid (Al/Zr (molar) = 1).

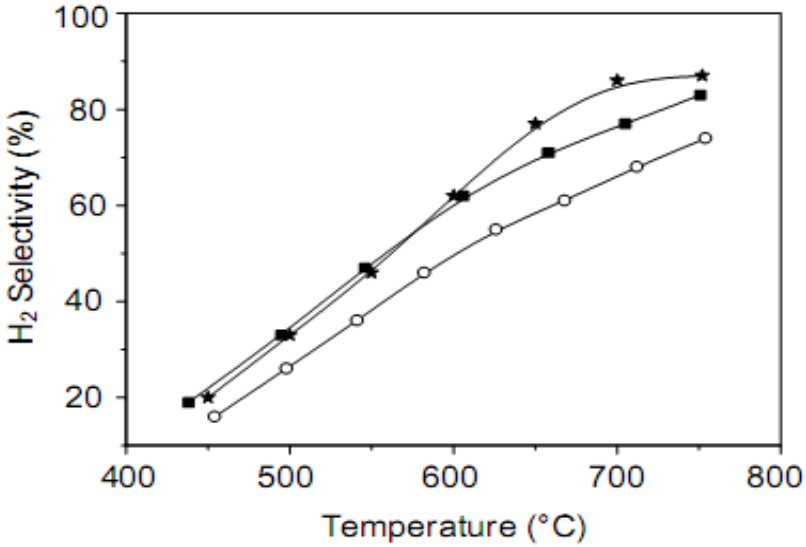

Figure 8. Hydrogen selectivity as a function of temperature in methane steam reforming over the catalysts. NAl sample (■): alumina-supported nickel. NZr sample (★): zirconia-supported nickel. NAZ sample (○): nickel supported on aluminum and zirconium solid (Al/Zr (molar) = 1).

The hydrogen selectivity as a function of temperature, during methane steam reforming (Figure 8), showed the same tendency as the conversion, the aluminum and zirconium-based catalyst showed the lowest selectivity. Moreover, the carbon monoxide selectivity as a function of temperature displayed similar profiles, as shown in Figure 9, but alumina-supported nickel showed the highest selectivities while the other catalysts showed similar values.

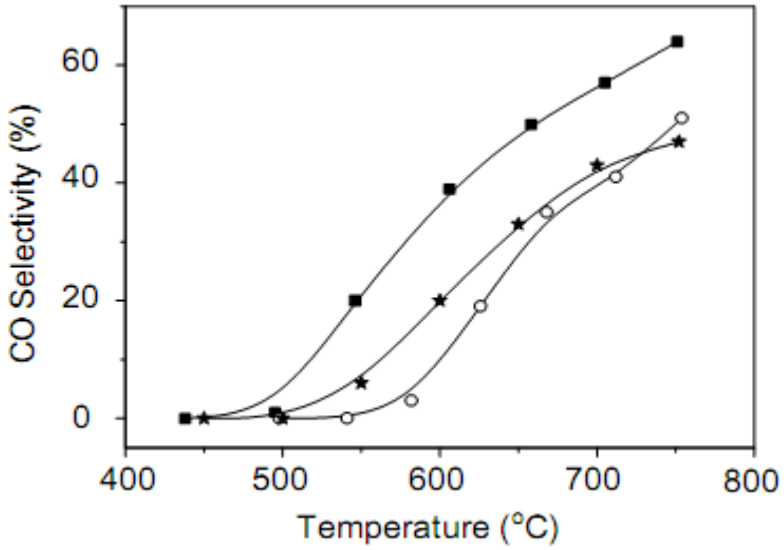

Figure 9. Carbon monoxide selectivity as a function of temperature in methane steam reforming over the catalysts. NAl sample (■): alumina-supported nickel. NZr sample (★): zirconia-supported nickel. NAZ sample (○): nickel supported on aluminum and zirconium solid (Al/Zr (molar) = 1).

It means that alumina-based catalyst has the lowest activity to WGSR (Eq. 2), followed by the zirconia-based solid and the aluminum and zirconium-containing sample. In fact, it can be seen, in Figure 10, the same tendency for WGSR. It can be noted that all catalysts showed 100 % of selectivity to carbon dioxide at low temperatures (below 550 ^{o}C), resulting in no carbon monoxide in the products. It indicates that all carbon monoxide produced reacted with steam by WGSR to produce carbon dioxide and hydrogen. However, the temperature increase causes a decrease in the activity of the catalysts towards WGSR, causing an increase of the amount of carbon monoxide, as shown in Figure 9. It can also be seen, from Figure 10, that the aluminum and zirconium-based catalyst is the most active in WGSR followed by zirconia-supported nickel and alumina-supported nickel. These results indicate that the addition of zirconium to alumina-supported nickel decreased the activity for methane steam reforming and favored the WGSR.

The values of H_2/CO ratio as a function of temperature, during steam reforming of methane on the catalysts, are shown in Figure 11. It can be noted that they decreased with increasing temperature with no significant differences in these values at temperatures higher than 650 °C. Below this temperature, the samples led to high values, which can be explained by the enhancement of the WGSR at low temperatures; at values lower than 500 ^{o}C, no carbon monoxide was detected because it was converted to hydrogen and carbon dioxide by WGSR. From the results, one can conclude that the H_2/CO ratio can be adjusted by the kind

of the support and by the reaction temperature. Thus, high pure hydrogen can be obtained at temperatures up to 550 ^{o}C, depending on the support.

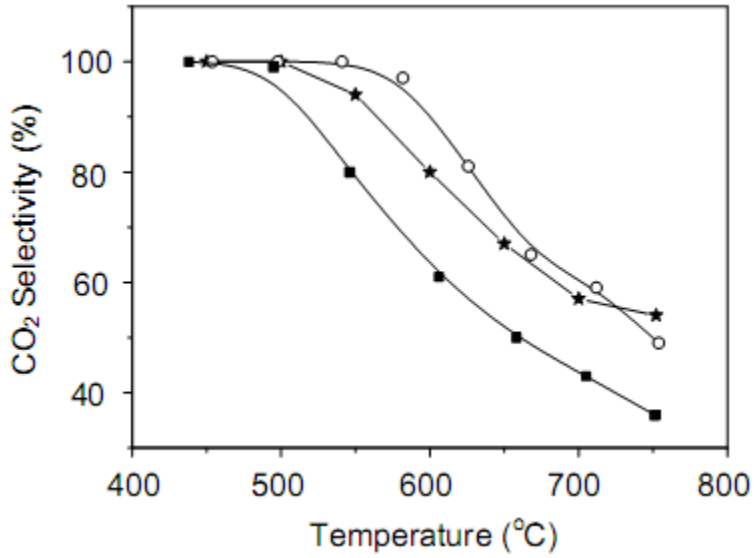

Figure 10. Selectivity to carbon dioxide as a function of temperature in methane steam reforming over the catalysts. NAl sample (■): alumina-supported nickel. NZr sample (★): zirconia-supported nickel. NAZ sample (○): nickel supported on an aluminum and zirconium-based solid (Al/Zr (molar) = 1).

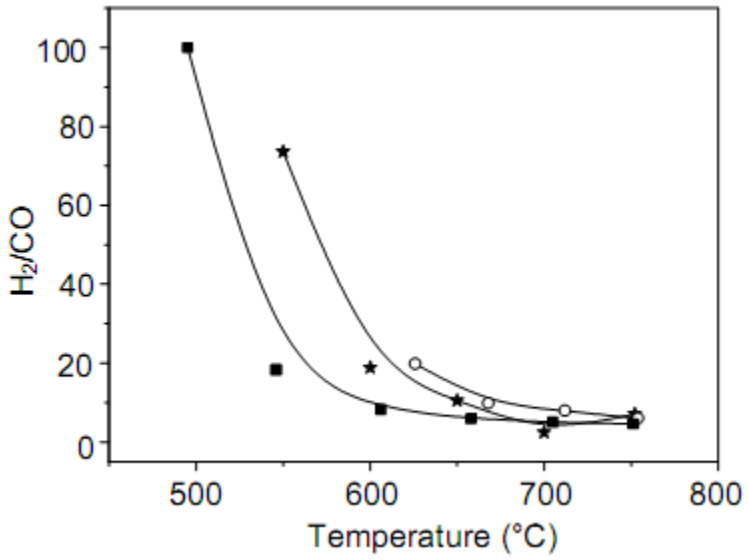

Figure 11. Hydrogen to carbon monoxide molar ratio as a function of temperature in methane steam reforming over the catalysts. NAl sample (■): alumina-supported nickel. NZr sample (★): zirconia-supported nickel. NAZ sample (○): nickel supported on aluminum and zirconium-based solid (Al/Zr (molar) = 1).

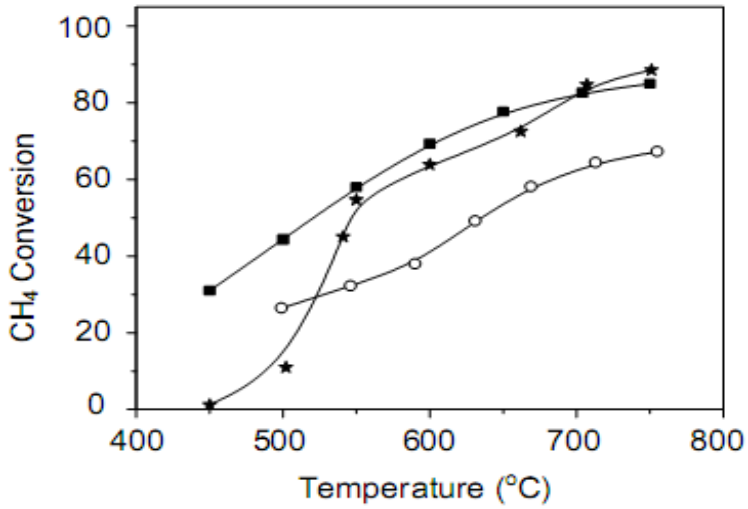

Figure 12. Methane conversion as a function of temperature in the autothermal reforming of methane over the catalysts. NAl sample (■): alumina-supported nickel. NZr sample (★): zirconia-supported nickel. NAZ sample (○): nickel supported on aluminum and zirconium-based solid (Al/Zr (molar) = 1). The percentage is missing: CH4 conversion (%).

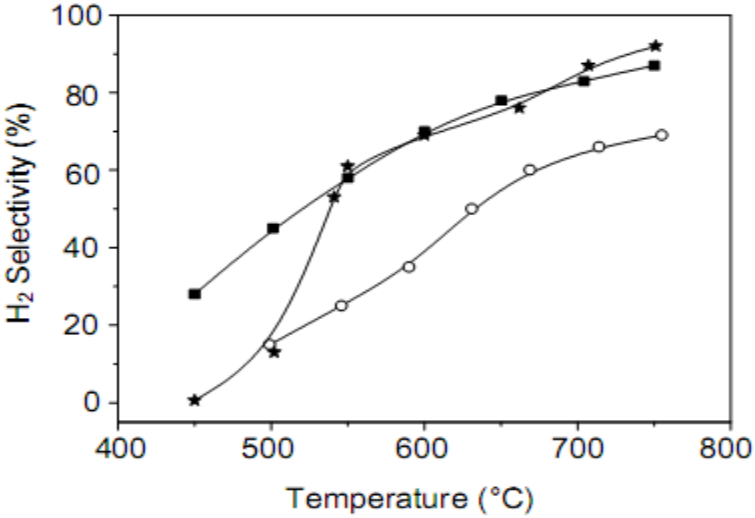

Figure 13. Hydrogen selectivity as a function of temperature in autothermal reforming of methane on the catalysts. NAl sample (■): alumina-supported nickel. NZr sample (★): zirconia-supported nickel. NAZ sample (○): nickel supported on aluminum and zirconium-based solid (Al/Zr (molar) = 1).

The catalysts showed similar performances for the autothermal reforming of methane, the conversion increased with temperature. From Figure 12, one can see that the aluminum and zirconium-containing catalyst was the least active while the others led to similar conversions at temperatures higher than 550 ^{o}C; below this temperature, zirconia-supported nickel was the least active catalyst. The curves of hydrogen selectivity (Figure 13), as well as those for carbon monoxide selectivity (Figure 14), showed similar tendencies as the conversion. It can be noted that the aluminum and zirconium-containing catalyst showed no carbon monoxide

selectivity at temperatures lower than 600 °C; zirconia-supported nickel showed the same behavior at temperatures lower than 500 °C, while alumina-supported nickel showed no selectivity to carbon monoxide only at 450 °C. It means that they led to the complete conversion of carbon monoxide produced in methane reforming to carbon dioxide and hydrogen by WGSR. The curves of carbon dioxide (Figure 15) show that the aluminum and zirconium-containing catalyst was the most active to WGSR, followed by the other catalysts that showed similar activities.

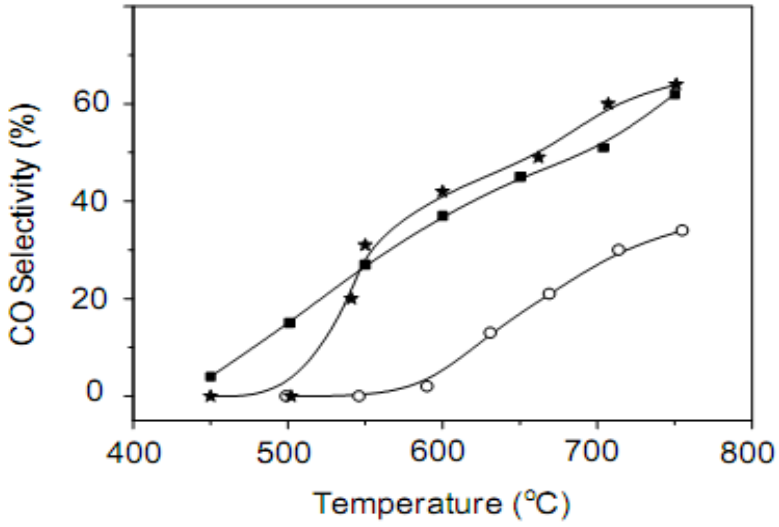

Figure 14. Selectivity to carbon monoxide as a function of temperature in the autothermal reforming of methane over the catalysts. NAl sample (■): alumina-supported nickel. NZr sample (★): zirconia-supported nickel. NAZ sample (○): nickel supported on aluminum and zirconium-based solid (Al/Zr (molar) = 1).

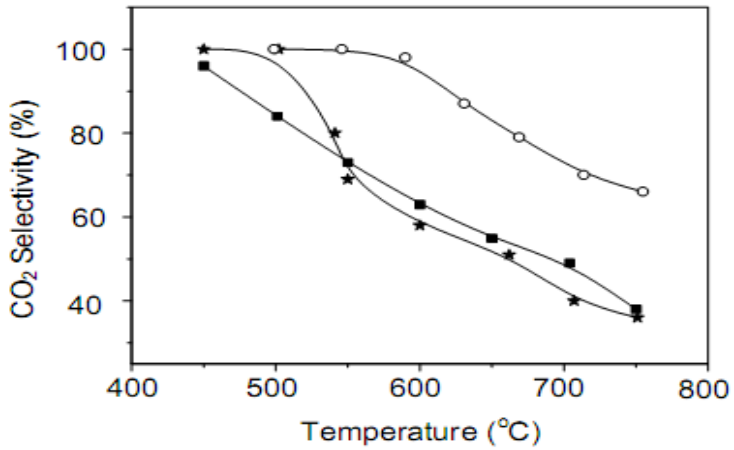

Figure 15. Selectivity to carbon dioxide as a function of temperature in autothermal reforming of methane on the catalysts. NAl sample (■): alumina-supported nickel. NZr sample (★): zirconia-supported nickel. NAZ sample (○): nickel supported on aluminum and zirconium-based solid (Al/Zr (molar) = 1).

Figure 16 shows the H_2/CO molar ratio for the catalysts in autothermal reforming. It can be noted that they decreased with the temperature increase; achieving values lower than six at around 750 ^oC, this can be ascribed to the highest activity of the catalysts to WGSR at low temperatures.

These results show that zirconia is a promising support to nickel-based catalysts to both steam reforming and autothermal reforming of methane, leading to performances close to alumina. The addition of high amounts of aluminum to zirconia (Al/Zr= 1) led to a decrease of activity and of hydrogen selectivity but is useful to adjust the H_2/CO ratio.

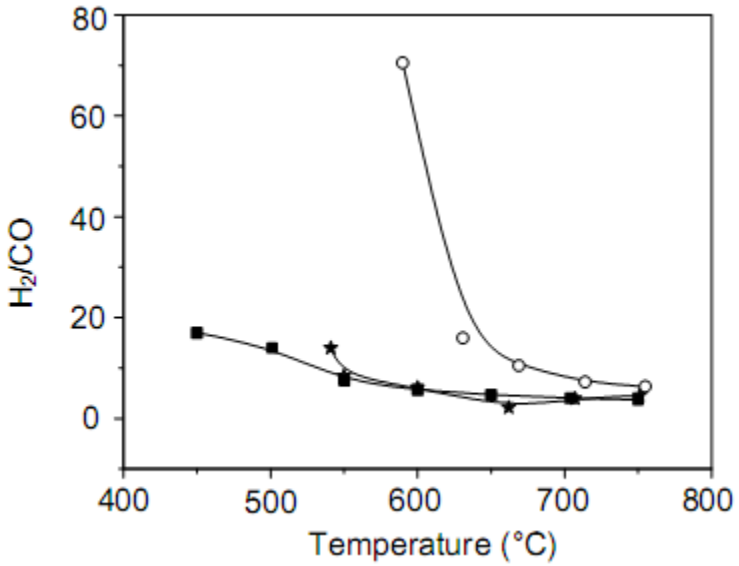

Figure 16. Hydrogen to carbon monoxide molar ratio as a function of temperature in autothermal reforming of methane on the catalysts. NAl sample (■): alumina-supported nickel. NZr sample (★): zirconia-supported nickel. NAZ sample (○): nickel supported on aluminum and zirconium-based solid (Al/Zr (molar) = 1).

CONCLUSION

Zirconia, alumina and aluminum and zirconium-based support (Al/Zr= 1) for nickel-based catalysts were compared, for both steam and autothermal reforming, in order to obtain efficient catalysts to produce hydrogen. Zirconia-supported nickel showed the monoclinic and tetragonal phases while alumina-supported nickel showed gamma-alumina structure; the aluminum and zirconium-based solid showed the tetragonal phase of zirconia and gamma-alumina, indicating that alumina stabilized the tetragonal phase. Nickel oxide (NiO) was found ~~for~~ in all catalysts. The addition of nickel to the supports caused a decrease in specific surface area, which was related to the pore blockage by the metal. Nickel was more reducible on zirconia than on alumina and showed an intermediate behavior on the mixed support. All catalysts were active in steam reforming and autothermal reforming of methane and the conversion increased with temperature. For both reactions, zirconia-supported nickel and alumina-supported nickel were the most active and selective to hydrogen, showing similar performances while the aluminum and zirconium-containing catalyst showed the worst

performance. These findings were related to the ability of zirconia in favoring the reduction of nickel particles while alumina provided high specific surface area; it seems that the highest specific surface area of alumina compensates the lower amounts of active sites produced in this catalysts, as compared to zirconia-supported nickel, resulting in catalysts with similar performances. The catalysts were also active in water gas shift reaction which occurred mainly at lower temperatures; alumina-supported nickel was the least active while the aluminum and zirconium-based catalyst was the most active. As whole, hydrogen selectivity was higher for autothermal reaction than for steam reforming, but it depended on the kind of support and on the reaction temperature. It can be concluded that zirconia is a promising support for nickel-based catalysts to produce hydrogen by methane steam reforming or by methane autothermal reforming. In addition, the H_2/CO ratio can be adjusted by the addition of alumina and by the reaction temperature.

REFERENCES

[1] Pompeo, F.; Gazzoli, D.; Nichio, N. Stability improvements of Ni/α-Al_2O_3 catalysts to obtain hydrogen from methane reforming. *Int. J. Hydrogen Energy* 2009, 34, 2260-2268.

[2] Cao, Y.; Wenju, W. Hydrogen-rich gas production for solid oxide fuel cell (SOFC) via partial oxidation of butanol: Thermodynamic analysis. *Int. J. Hydrogen Energy* 2010, 35, 13280-13289.

[3] Abbas, H.; Daud, W. Hydrogen Production by methane decomposition: A review. *Int. J. Hydrogen Energy* 2010, 35, 1160-1190.

[4] Lunsford, J. H. Catalytic conversion of methane to more useful chemicals and fuels: a challenge for the 21st century. *Catal. Today* 2000, 63,165 – 174.

[5] Rodrígues-Castellón, E.; Jiménes-Lopez, A.; Eliche-Quesada, D. Nickel and cobalt promoted tungsten and molybdenum sulfide mesoporous catalysts for hydrodesulfurization. *Fuel* 2008, 87, 1195-1206.

[6] Ramachandran, R.; Menon, R. An overview of industrial uses of hydrogen. *Int. J. Hydrogen Energy* 1998, 23, 523-528.

[7] Eliezer, D.; Eliaz, N.; senkov, O. N.; Froes, F. Positive effects of hydrogen in metais. *Mat. Sci. Eng*. A 2000, A280, 220-224.

[8] Rostrup – Nielsen, J. R. New aspects of syngas production and use. *Catal. Today* 2000, 63, 159–164.

[9] Holladay, J.D.; Hu. J.; King, D.L.; Wang, Y. An overview of hydrogen production technologies. *Catal. Today* 2009, 139, 244–260.

[10] Lima, S.P.; Vicentini, V.; Fierro, J.L.G.; Rangel, M.C. Effect of aluminum on the properties of lanthana-supported nickel catalysts. *Catal. Today* 2008, 133-135, 925–930.

[11] Berrocal, G.P.; Silva, A; Assaf, J.M.; Albornoz, A.; Rangel, M.C. Novel supports for nickel-based catalysts for the partial oxidation of methane. *Catal. Today* 2010, 149, 240–247.

[12] Dias, J.A.C.; Assaf, J.M. Autothermal reforming of methane over Ni/γ-Al_2O_3 promoted with Pd The effect of the Pd source in activity, temperature profile of reactor and in ignition. *Appl. Catal. A: Gen*. 2008, 334, 243 – 250.

[13] Araujo, G.C.; Lima, S.M.; Assaf, J.M.; Peña, M.A.; Fierro, J.L.G.; Rangel. M.C. Catalytic evaluation of perovskite-type oxide $LaNi_{1-x}Ru_xO_3$ in methane dry reforming. *Catal. Today* 2008, 133, 129-135.

[14] Pereira, A. L. C.; González-Carballo, J. M.; Pérez-Alonso, F. J.; Rojas, S.; Fierro, J. L.; Rangel. M. R. Effect of the mesostructuration of the beta zeolite support on the properties of cobalt catalysts for Fischer-Tropsch synthesis. *Top. Catal.* 54 (2011) 179-189.

[15] Araujo, G.; Lima, S.; Rangel, M. C.; Parola, V.; Pena, M. A.; Fierro, J. L. G. Characterization of precursors and reactivity of $LaNi_{1-x}Co_xO_3$ for the partial oxidation of methane. *Catal. Today* 2005, 107, 906-912.

[16] Cavallaro, S.; Frani, S. V. Syngas and electricity production by an integrated autothermal reforming/molten carbonate fuel cell system. *J. Power Sources* 1998, 76, 190.

[17] Armor, J. The multiple roles for catalysis in the production of H_2. *Appl. Catal*. A 1999, 176, 159 – 176.

[18] Hou, Z.; Chen, P. Fang, H.; Zheng, X.; Ashima, T. Production of synthesis gas via methane reforming with CO2 on noble metals and small amount of noble-(Rh-) promoted Ni catalysts. *Int. J. Hydrogen Energy* 2006, 31, 555 – 561.

[19] Carvalho, L. S.; Martins, A. R.; Reyes, P.; Oportus, M.; Albornoz, A.; Vicentini, V.; Rangel, M. C. Preparation and characterization of Ru/MgO-Al_2O_3 catalysts for methane steam reforming. *Catal. Today* 2009, 142, 52-60.

[20] Moura, J. S.; Souza, M. O.; Rangel, M. C. Effect of magnesium on the properties of nickel and lanthanum-based catalysts in steam reforming. Fuel 2008, 87, 3627-3630.

[21] Muradov, N. Emission-free fuel reformers for mobile and portable fuel cell application. *J. Power Sources* 2003, 118, 320-324.

[22] Hammer, T.; Kappes,T.; Baldauf, M. Plasma catalytic hybrid processes: gas discharge initiation and plasma activation of catalytic processes. *Catal. Today* 2004, 89, 5-14.

[23] Metkemeijer, R.; Achard, P. Ammonia as a feedstock for a hydrogen fuel cell; reformer and fuel cell behaviour. *J. Power Sources* 1994, 49, 271–282.

[24] Rostrup – Nielsen, J. R. Manufacture of Hydrogen. *Catal. Today* 2005, 106, 293–296.

[25] Twigg, M.V. Catalyst Handbook, 2° Edition. Mason Publishing, London, 1997.

[26] Therdthianwong, S.; Therdthianwong, A.; Siangchin, C.; Yongprapat, S. Synthesis gas production from reforming of methane over Ni/Al2O3 stabilized by ZrO_2. *Int. J. Hydrogen Energy* 2008, 33, 991-999.

[27] Rangel, M. C.; Souza, Oliveira da Guarda, M.; Sodré, D.; Silva, A. L. M.; Ramos, M.; S.; Assaf, J. M. Partial oxidation of methane over zirconia and magnesia-supported ruthenium and rhodium catalysts. In: Adorjan Kurucz; Izsak Bencik. (Org.). Syngas: *Production Methods, Post Treatment and Economics*. Hauppauge: Nova Science Publishers, Inc., 2009, 395-408.

[28] Lanza, R; Järås, S. G., Canu, P. Partial oxidation of methane over supported ruthenium catalysts. *Appl. Catal. A: Gen*. 2007, 325, 57-67.

[29] Lødeng, R.; Bjørgum, E.; Bjørn C. E.; Eilertsen, J.; Holmen, A.; Krogh, M. R.; Rytter, E. Catalytic partial oxidation of CH4 to H2 over cobalt catalysts at moderate temperatures. *Appl. Catal. A:Gen*. 2007, 333, 11 – 23.

[30] Wang, Y. H.; Zhang, J. C. Hydrogen production on Ni-Pd-Ce/γ-Al2O3 catalyst by partial oxidation and steam reforming of hydrocarbons for potential application in fuel cells. *Fuel* 2005, 84, 1926 – 1932.

[31] Peña, M.A.; Gomez, J.P.; Fierro, J.L.G. New catalytic routes for syngas and hydrogen production. *Appl. Catal. A: Gen*. 1996, 144, 7–57.

[32] Nezhad, M.Z.; Rowshanzami, S.; Eikani, M.H. Autothermal reforming of methane to synthesis gas: modeling and simulation, Int. J. Hydrogen Energy 2009, 34, 1292–1300.

[33] Mishra, D.; Anand, S.; Panda, R.; Das, R. Hydrothermal preparation and characterization of boehmites. *Mater. Lett*. 2000, 42, 38–45.

[34] Perego, C.; Villa, P. Catalyst preparation methods. *Catal. Today* 1997, 34, 281-305.

[35] Caruso, R.; Sanctis, O.; Macías-García, A.; Benavidez, E.; Mintzer, S. Influence of pH value and solvent utilized in the sol–gel synthesis on properties of derived ZrO_2 powders. *J. Mater. Process. Tech*. 2004, 152, 299–303.

[36] Yu, G.; Zhu, L,; Wang, X.; Liu, J.; Xu, D. Fabrication of silica-supported ZrO_2 mesoporous fibers with high thermal stability by sol-gel method though a controlled hydrolysis-condensation process. *Microporous Mesoporous Mater*. 2010, 130, 189–196.

[37] Nyquist, R.A.; Kagel, R. O. *Infrared spectra of inorganic compounds*. Academic Press, Orlando, 1971.

[38] Hubert, J.; Asha K.. V.; Aruldhas, G.; Damodaran, A. D.; Warrier, K. FTIR as a tool to study high-temperature phase formation in sol–gel aluminum titanate. *J. Solid State Chem.* 1997, 131, 181-184.

[39] Virgens, C. F. das; Rangel, M. C. Influence of the Preparation Method on the Textural Properties of Zirconia . *React. Kinet. Catal. L*. 2005, 84, 183-188.

[40] Webb, P.A.; Orr, C. *Analytical methods in fine particle technology*, Micromeritics Instruments Coorporation, Norcross, 1997.

[41] Wang, S.; Lu, G. CO2 reforming of methane of Ni catalysts: effects of the support phase and preparation techniques. *Appl. Catal. B: Environ*. 1998, 16, 269–277.

[42] Sanchez, M.C.; Navarro, R.M.; Fierro, J.LG. Ethanol steam reforming over Ni/M_xO_y-Al_2O_3 (M=Ce, La, Zr and Mg) catalysts: influence of support on the hydrogen production. *Int. J. Hydrogen Energy* 2007, 32, 1462-1471.